Bioorganic & Medicinal Chemistry Letters 20 (2010) 4182–4187

Contents lists available at ScienceDirect

Bioorganic & Medicinal Chemistry Letters

journal homepage: www.elsevier.com/locate/bmcl

Interaction of aminoadamantane derivatives with the influenza A virus M2 channel-Docking using a pore blocking model

Stelios Eleftheratos [a], Philip Spearpoint [c], Gabriella Ortore [b], Antonios Kolocouris [a,*], Adriano Martinelli [b], Stephen Martin [c], Alan Hay [c]

[a] Faculty of Pharmacy, Department of Pharmaceutical Chemistry, University of Athens, Panepistimioupolis-Zografou, 15771 Athens, Greece
[b] Dipartimento di Scienze Farmaceutiche, UniVersità di Pisa, Via Bonanno 6, 56126 Pisa, Italy
[c] MRC National Institute for Medical Research,The Ridgeway, Mill Hill, London NW7 1AA, UK

ARTICLE INFO

Article history:
Received 8 April 2010
Revised 11 May 2010
Accepted 13 May 2010
Available online 20 May 2010

Keywords:
Influenza A
M2TM blockers
Aminoadamatanes
Amantadine
Rimantadine
Binding constants
Trp fluorescence
Pore-blocking model
Docking calculations

ABSTRACT

Interaction of aminoadamantanes with the influenza A virus M2 proton channel was analyzed by docking simulations of a series of synthetic aminoadamantane derivatives, of differing binding affinity, into the crystal structure of the transmembrane (M2TM) pore. The pore blocking model tested in the 'gas phase' describes qualitatively the changes on the relative binding affinities of the compounds (although a series of highly hydrophobic ligands which seem to have little capacity for different specific interactions with their receptor). The docking calculations predicted poses in which the adamantane ring is surrounded mainly by the alkyl side chains of Val27 or Ala30 and the ligand's amino group is generally hydrogen bonded with hydroxyls of Ser31 or carbonyls of Val27 or carbonyls of Ala30, the former (Ser31) being the most stable and most frequently observed. The binding of the ligand is a compromise between hydrogen bonding ability, which is elevated by a primary amino group, and apolar interactions, which are increased by the ability of the lipophilic moiety to adequately fill a hydrophobic pocket within the M2TM pore. A delicate balance of these hydrophobic contributions is required for optimal interaction.

Influenza presents a severe threat to public health. More casualties were inflicted in Europe in the 20th century by influenza than any other infectious disease.[1] The 2009 pandemic influenza A virus of the subtype H1N1 although clinically has caused mainly mild disease similar to seasonal influenza, it has been responsible for severe disease and more than 10,000 fatalities were recorded during 2009.[2,3] The 'terrible experience' of the 1918 flu pandemic,[1] which killed approximately 600,000 people in the United States alone, was preceded by a mild 'herald' wave in the spring, and there is continuing concern that the pandemic H1N1 2009 virus might mutate into a more virulent form.

The M2 protein of influenza A viruses is the target of one of two classes of anti-influenza drugs that have been used to help control influenza infections.[4] Amantadine **4** (Am **4**, Scheme 1) was the first anti-influenza drug to be developed. It inhibits the function of the M2 proton channel of influenza A viruses involved in virus entry and uncoating.[5]

Drug resistance mutations cause amino acid substitutions in the M2 transmembrane domain (M2TM) and most naturally arising mutations have altered residues Val27, Ala30 and Ser31.[5a,b] Neither influenza B virus replication nor BM2 ion channel activity are inhibited by the drug. The X-ray crystallographic atomic structure of the A/M2 TM domain with and without bound amantadine was recently published.[6] As predicted from earlier biochemical and ssNMR studies[7,8] the recent high-resolution structural information show that the overall architecture of the TM domain is a four-helix bundle and the data confirm predictions that His37 forms the pH sensor and Trp41 the channel gate.[9,10] Early neutron diffraction[11] and early[12] and recent MD simulations[13,14] both supported amantadine binding inside the M2TM pore towards the N-terminus of the helical bundle. In the crystal structure of the amantadine–M2TM complex, determined with a 1.3:1 protein/amantadine molar ratio, one drug molecule binds each M2 tetramer in the pore[6] (which is consistent with the one-drug-per-channel stoichiometry of amantadine inhibition[15]) and the drug is surrounded by residues Val27, Ala30, Ser31, in which single substitutions cause amantadine resistance.[5a,b] Recent ssNMR data showed that the M2TM conformation is most perturbed by amantadine at Ser31, strongly suggesting the drug binds near Ser31.[16]

In order to design effective new inhibitors of virus replication and those active against amantadine-resistant mutants, the mode of interaction of the class of compounds with their receptor should

* Corresponding author. Tel.: +30 1 210 7274834 (office), +30 1 210 7274315 (lab); fax: +30 1 210 7274747.
E-mail address: ankol@pharm.uoa.gr (A. Kolocouris).

0960-894X/$ - see front matter © 2010 Elsevier Ltd. All rights reserved.
doi:10.1016/j.bmcl.2010.05.049

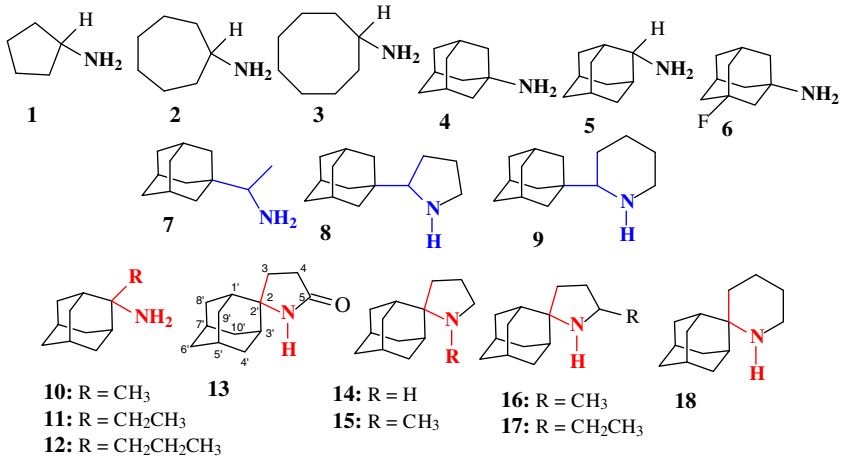

Scheme 1. Structures of the compounds used in this work. The coloured bonds indicate structural similarities inside the relevant series.

be systematically examined at the molecular level. Although we have tested the in vitro potencies of several synthetic aminoadamantane derivatives in cell culture[17–19] we have only recently applied procedures that measure directly changes in physicochemical properties of the target protein as a result of drug–receptor interaction. These include an examination of how the molecules interact with the transmembrane domain of the M2 channel protein, using suitable probe molecules and NMR spectroscopy,[20] and measurement of the affinities of ligand binding[19,21] using an assay based on the inhibition of quenching of Trp41 fluorescence by His37 protonation in the M2 channel pore;[21] in the latter case the binding constants of compounds **4**, **5**, **10**–**12**, **14**, **18** (Scheme 1) were determined and reported in a preliminary work.[19] In this work the binding affinities to M2 protein of the compounds shown in Scheme 1 are reported. Since a binding site model should be able to explain the relative affinities of the ligands, a pore blocking model was tested[22] in this preliminary work by applying docking simulations to a series of synthetic aminoadamantane ligands[23] (Scheme 1).

According to previous representation of the pore blocking model and the recent X-ray and ssNMR structure of the M2TM–Am **4** complex[6] it seems that the drug's ammonium group is linked directly or indirectly (through a chain of water molecules) with residues His37 or Ser31; Ser31 may be a likely H-bonding acceptor given that an S31N mutation is responsible for most amantadine resistance.[24] Preliminary data indicate that compounds **8**, **10**, **14**, **15** and **18** cause mainly S31N substitutions.[25] The interactions between M2TM and the ligands in the aminoadamantane series **1**–**18** will be analyzed below to investigate this H-bonding interaction. In addition, compounds **8**, **9**, **10**–**18** possess a significant apolar part, in addition to adamantane, that may interact through van der Waals forces with a suitable lipophilic pocket of the M2TM pore, such as formed by the alkyl side chains of the pore lining residues Val27 and Ala30. They were examined to determine how an increase in the lipophilic volume around the nitrogen influences interactions of the compounds and their affinity for the M2TM.

This is the first work on the docking analysis description of experimental SAR studies based on the measured binding affinities to M2 protein of a series of lipophilic amine derivatives.

Binding studies: The binding affinities of compounds **1**–**18** (Scheme 1) for purified M2 protein of the influenza Weybridge strain are depicted in Table 1.

The first two lines of Scheme 1 depict lipophilic amines with different cycloalkyl groups, cyclopentanamine **1**, cycloheptanamine **2**, cyclooctanamine **3**, 1-adamantanamine or amantadine **4** (Am **4**), 2-adamantanamine (2-amantadine) **5** and 3-fluoro-1-adamantanamine **6**.

Table 1
Binding constants[a] of some aminoadamantane derivatives[b] against influenza A M2 protein[c]

Compound	K_d (μM)
1	No effect
2	16.2
3	1.83
4 (Amantadine)	0.32
5 (2-Amantadine)	2.36
6	4.86
7 (Rimantadine)	0.016
8	0.51
9	1.51
10	3.60
11	6.70
12	8.71
13	1.49
14	1.16
15	2.93
16	1.50
17	5.58
18	0.39

[a] Binding constants were obtained from the kinetics of inhibition, under equilibrium conditions, of the quenching of Trp41 fluorescence by His37 protonation.
[b] The amines **1**–**5** and **7**–**18** were hydrochloride salts; **6** and **17** were acetate and fumarate salts, respectively (see Supplementary data).
[c] Purified M2 of the influenza Weybridge (H7N7) strain, expressed in *E. coli*.

Of the cycloalkanamines **1**–**3**, cyclopentanamine **1** is inactive and cyclooctanamine **3** had the highest affinity; it is remarkable that the small increase in ring size from cycloheptanamine **2** (K_d = 16.2 μM) to cyclooctanamine **3** (K_d = 1.83 μM) results in a ~9-fold increase in affinity suggesting the importance of hydrophobic interactions with the binding pocket. When the symmetric 1-adamantyl group (C_{3v} symmetry) was attached instead of the cyclooctyl group, a sixfold increase in binding affinity was observed (**4**, K_d = 0.32 μM). Replacement of the 1-adamantyl group by the less symmetric 2-adamantyl group (D_{3d} symmetry) resulted in a sevenfold smaller binding constant (**5**, K_d = 2.36 μM). Again the difference in binding affinity is remarkable and it appears therefore that amantadine **4** has a more favourable orientation than 2-amantadine **5** inside the M2TM pore. The effect of inserting a fluorine group at the bridgehead position of amantadine **4** (compound **6**) is of interest since it resulted in a 15-fold smaller binding constant, which can be explained in part by the effect of the fluorine atom in reducing the H-bond donor ability of the ammonium group.

Addition of a –CH(CH_3)– bridge in rimantadine **7** between the 1-adamantyl and amino groups in **4** resulted in a 20-fold higher binding affinity compared to that of amantadine **4**, the highest binding efficacy in the series of the compounds tested, with a binding constant in the nanomolar range (K_d = 0.016 μM). Since rimantadine **7** is likely to have a similar lipophilicity as several of the other compounds (depicted in Scheme 1), its strikingly higher binding affinity must be due to more delicate interactions.

For the two heterocyclic rimantadine analogues, inclusion of the amino group of rimantadine in the pyrrolidine ring in compound **8** resulted in a 32-fold reduction of binding strength (K_d = 0.51 μM), and a further threefold reduction for piperidine **9** (K_d = 1.51 μM). Our curiosity to explain large differences in affinity between rimantadine **7** and the aminoadamantane series of compounds depicted in Scheme 1 triggers in part the calculations using the pore blocking model, which will be described in the next section.

To study the effect of attaching a carbon chain at the C-2 position of 2-amantadine **5**, compounds **10**–**18** were synthesized. In a general sense, compounds **14** and **18**, for example, are 2-adamantanamines substituted at the 2-position with a carbon chain. Simplification of this structure leads to the simpler 2-alkyl-2-adamantanamines **10**–**12**;[19] the simplest structure in that series is that of the 2-methyl-2-adamantanamine **10**.

Spiropiperidine **18** with a K_d of 0.39 μM, similar as to that of Am **4**, had a sixfold higher affinity than **5**, while reduction in the ring size by one methylene, in spiropyrrolidine **14**, caused a threefold reduction in binding affinity (K_d = 1.16 μM), but twofold higher than that of 2-amantadine **5**. It is noted that spiropyrrolidine **14**[17,18a,b] and spiropiperidine **18**[17,18a,c] are two of the most active anti-influenza A virus M2 agents ever synthesized after the amantadine **1** and rimantadine **2** drugs discovery; the in vitro selectivity index of the spiro[piperidine-2,2′-adamantane] **18** (SI >1034) is, after rimantadine, the highest among synthetic aminoadamantanes or other cage structure amines tested till now (see Ref. 6 of Supplementary data).

The lactam precursor **13** of the latter **14** had a similar binding affinity (K_d = 1.49 μM), suggesting that an amide group can effectively replace the amino group for favourable interactions with the receptor. Since spiropyrrolidine **14** and spiropiperidine **18** can be considered to be 2-alkyl-2-aminoadamantanes, the effects of attaching simple alkyl groups at the 2-position of **5** was unexpected. They did not result in more stable complexes, as for **14** and **18**, the methyl, ethyl and *n*-propyl substitutions (compounds **10**, **11** and **12**, respectively) reduced the binding affinity by 1.5-, 2.8- and 3.7-fold, respectively, with respect to 2-amantadine **5**. Derivatives **15**, **16**,[18g] and **17** were included to check how the slight increase in the lipophilic volume of compound **14**, by adding a methyl or ethyl group into the 5-position of the pyrrolidine ring will affect binding affinity. Thus, N-methylation of the pyrrolidine **14** reduced by 2.5-fold the binding constant of compound **15** (K_d = 2.93 μM). Addition of a methyl group at the 5-position of the pyrrolidine scaffold of compound **14** to produce compound **16**, which is isomeric to the spiropiperidine **18**, did not affect binding significantly, while further lengthening of the 5-alkyl group, by only one methylene, reduced considerably the affinity of the 5-ethyl derivative **17** (K_d = 5.59 μM). It seems that the mean molecular volumes of compounds **16**, **17** may have reached the dimensions of the relevant area in the M2 channel; these changes in binding affinity caused by small alterations of ligands structure are really valuable for checking the quality of the docking calculations using the pore blocking model. These findings suggest that the rigid carbon framework of pyrrolidine and piperidine rings in compounds **14** and **18** fit better, than a free rotating group, into a lipophilic pocket in the M2 receptor. Interestingly, in a recent publication, it has been proposed that when designing new M2 channel blockers it may be necessary to increase the drug size, since such compounds may also be active against amantadine-resistant viruses.[26]

Computational chemistry—Docking calculations: Current scoring functions are deficient in predicting accurately the binding affinities changes of related compounds from a known active series.[27] However, these docking algorithms and scoring functions are widely used in the literature to obtain a qualitative description of the drug–protein complex. This 'chemical' interpretation must not be underestimated, because it can help in understanding how apolar and H-bonding interactions can be changed with small modifications of the drug structure.

Thus, the present calculations cannot be correlated directly with free energy binding changes as resulted from the experimental binding constants. This preliminary study tested a pore blocking model to rationalize qualitatively the experimental SAR studies, that is, to account roughly for different molecular interactions between members of a series of aminoadamantane derivatives and the influenza virus A M2TM channel pore. The docking of compounds **1**–**18** (Scheme 1) into the M2TM was based on the crystal structure of a M2TM–Am **4** complex (PDB code 3c9j). Protein structure was prepared for docking using MAESTRO/MACROMODEL program. Docking calculations were performed using GOLD 4.1 and AUTODOCK 4 software (see Supplementary data). The X-ray structure, obtained at pH 5.3 to 3.5 Å resolution,[6] was of a 25 residues membrane-spanning peptide S22-L46 of the M2 tetramer. Its sequence, SSDPLVVAASIIAILHLILWILDRL, incorporating a G34A mutation, differed in the substitution F38L from the sequence of the full length M2 protein[21] used to determine the binding constants, which provide guiding parameters to understand basic similarities and differences in the modes of the ligand binding. The scoring functions used in GOLD (GoldScore, ChemScore and ASP) and that implemented in AUTODOCK 4 gave similar results.

Figure 1 includes illustrations of the best docking poses for some representative ligands inside the M2TM pore. In each complex the adamantane and additional lipophilic moiety of the ligand fits in a symmetrical hydrophobic pocket, which includes the apolar level HL1 defined by a ring of four Val27 isopropyl groups, the apolar level HL2 defined by a ring of four Ala30 methyl groups, and level HL3 corresponding to Ala34 residues (Fig. 1), while the ammonium group of the ligand interacts mainly with hydroxyls of Ser31 or hydroxyls of Ser31 and a carbonyl of Val27 or less frequently with the carbonyl of Ala30. After analyzing the results of the docking problem with GOLD and AUTODOCK 4 and the implemented scoring functions (see Supplementary data), the details of the mean docking interactions of the ligands examined are described below.

The X-ray structure[6] locates amantadine **4** towards the N-terminus of the M2TM surrounded roughly by the Val27, Ala30, Ser31 and Ala or Gly34 residues, that are mutated[5a,b] in natural and cell culture-selected amantadine-resistant viruses,[24,25] and suggests hydrogen bonding with a site deeper than Ser31 towards the C-terminal end; it is proposed that in this structure amantadine long axis is parallel to the pore axis and the amino group points to the C-terminal end. It should be emphasized that the exact position of the ligand cannot be extracted from the X-ray structure because of the 3.5 Å resolution.[6] Using these coordinates the docking calculations predicted poses in which the adamantane ring is surrounded mainly by Ala30 and the drug C–N bond axis is inclined with respect to the pore axis and oriented towards the N-terminal end of the pore; the ammonium group is hydrogen bonded to Ser31 hydroxyls[28] of two adjacent chains, and a Val27 carbonyl on the same chain as one of the two H-bonded Ser31 residues (SerC31, SerD31 and ValC27, Fig. 1b). After energy minimization of the best docking pose using either OPLS-2005 or force field AMBER* (implemented with Maestro) only the N^+–H···O–Ser31 hydrogen bonded contact remains stable. This drug position is

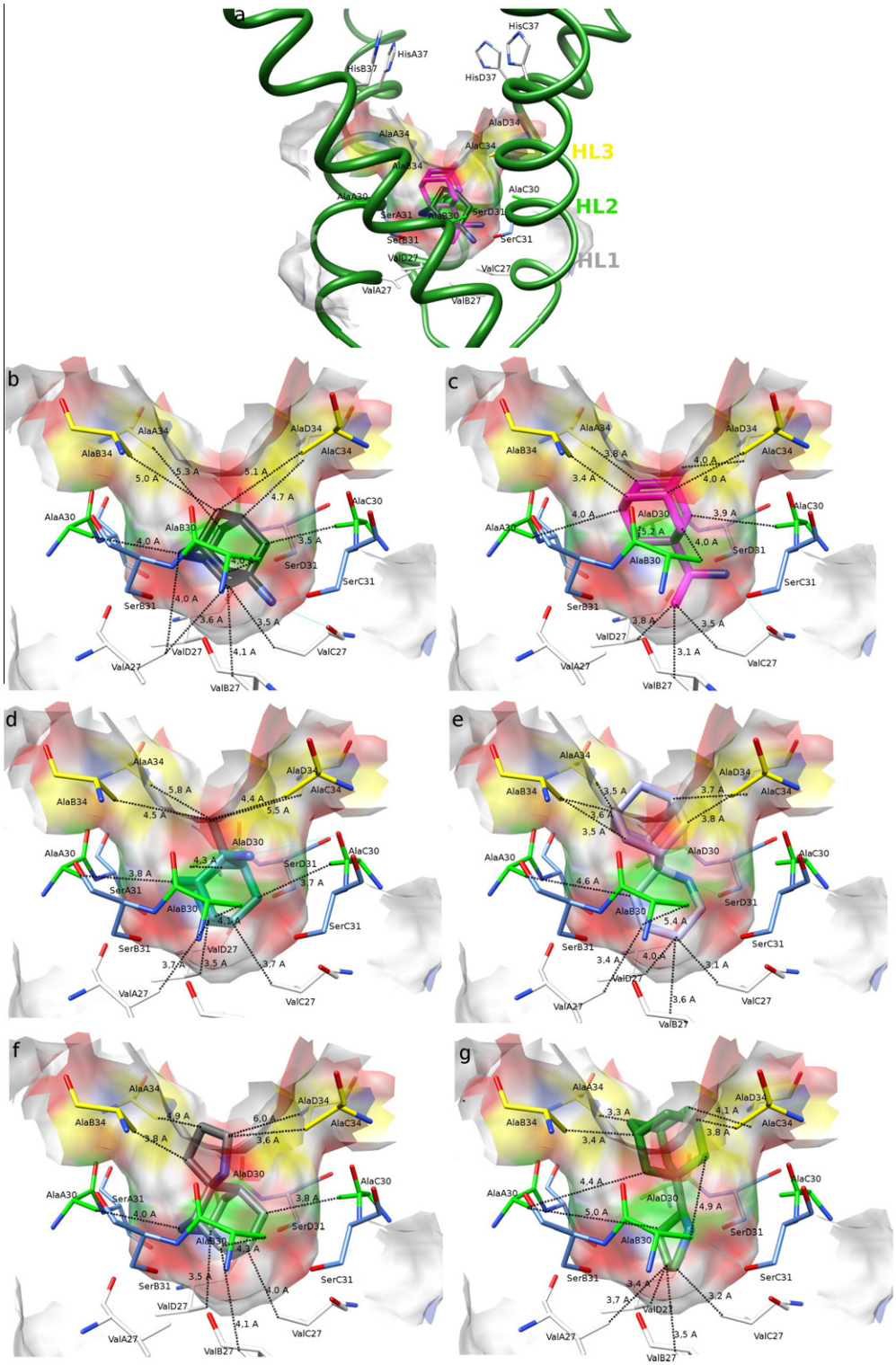

Figure 1. Illustration of preferable docking poses for representative aminoadamantane ligands included in Scheme 1.

consistent with recent ssNMR data which indicate that Ser31 is the site of the largest chemical shift perturbation on binding amantadine.[16]

The binding constant of compounds **8** and **9** were reduced by 31-fold and 94-fold, respectively, compared to that of rimantadine **7**. Compounds **8** and **9** are cyclic rimantadine analogues in which the amino group is included in pyrrolidine or piperidine rings, which represent additional lipophilic moieties. These heterocyclic rings are larger than the CH–CH_3 in rimantadine and these molecules moved higher from the N-end to the wider C-end of the pore. In Figure 1g it is shown that the ammonium group of the pyrrolidine derivative **8** points to the N-terminal end being hydrogen bonded with the SerC31 hydroxyl group and the adamantane ring is located between Ala30 and Ala34 residues and the nitrogen heterocycle is oriented between Ser31 and Val27 residues. It is straightforward that the primary amino group of rimantadine **7**

is capable of stronger hydrogen bonding interactions (three hydrogen bonding interactions with two Ser31 hydroxyl groups and one Val27 carbonyl group) than the crowded secondary amino group of the bulky rimantadine analogues **8**, **9** (one hydrogen bonding interaction with a Ser31 hydroxyl group) increasing considerably the stability of the complex. Furthermore, the second apolar moiety around nitrogen, in addition to adamantane ring, for compounds **8**, **9** and other members in aminoadamantane series (like **10**–**18**) seems to impair complex stability through favouring a fluctuation of the ligand inside the M2TM pore; a significant part of the docking problem solutions suggest that both the lipophilic parts, and thus also the amino group, can interact favourably and orient either to the C-end or the N-end of the pore.

As was noted in the introduction compounds **10**–**12** and **14**, **18** are 2-alkyl-2-adamantanamine analogues. The docking analysis provide a description of the different mean interactions responsible for the lower affinities of compounds **10**–**12** compared to **4**. The calculations located compounds **10**–**12** in positions similar to that of compound **4**. However, by increasing the length of the alkyl chain the alkyl- and amino-groups favour an orientation towards the C-end of the pore. The ammonium group of compound **10** forms a hydrogen bond with AlaC30 carbonyl group (Fig. 1d) or SerC31 and the apolar segments (adamantane ring and alkyl group) are placed to a distance of about 4 Å near Val27 and Ala30 alkyl side chains (residues of chains A, C, D in the figure). Compounds **11** and **12** are positioned in a less favourable docking by moving their aliphatic substituent in the wide area of the pore and their mean molecular volumes reach the dimensions of the pore cavity. Compared to compounds **14** or **18** the binding efficacy decreased substantially, suggesting the presence of a complementary site for pyrrolidine or piperidine rings, respectively, which cannot be occupied favourably by ethyl or *n*-propyl groups.

In fact, in spiropiperidine **18** the significant additional apolar segment, that is, the piperidine ring, increase the lipophilic volume such that the molecules move slightly toward the C-end of the pore, with adamantane ring covering the space between Ala34 and Ala30 and piperidine ring filling the space between Val27 and Ala30; the complex is stabilized through hydrogen bonding with one Ser31 hydroxyl group (SerD31, Fig. 1e). The calculations locate spiropyrrolidine **14** in orientation similar to that of compound **10** (Fig. 1d) in the binding site, but the increased lipophilic volume of compound **14** as regards **10** move the molecule toward the C-end of the pore allowing pyrrolidine ring to cover the space between Ala34 and Ala30 and to form a hydrogen bond with AlaB30 (Fig. 1f) or SerC31. The greater binding affinity of the piperidine analogue **18** over **14** may be the result of the more stabilizing enthalpic van der Waals interactions with Ala34 side chains, corresponding to distances of about 3.6 and 4.6 Å, respectively. As a result of the additional alkyl group attached to C5 position of pyrrolidine ring of compound **14**, compounds **16**, **17** did not fit well inside the pore; the substitution moves the pyrrolidine ring hampering hydrogen bonding and reducing binding affinity. The effect is more pronounced for the 5-ethyl derivative **22** where the ammonium group is pointed to the wider C-end of the pore without any H-bonded interaction. It seems that molecules **14** and **18** match more closely the dimensions of the pore in the area of the N-end.

Lactam **13**, the synthetic precursor of compound **14**, binds in the same orientation to that of **18** having weaker lipophilic interactions in the area between Val27 and Ala30 due to the more polar lactam ring which serves a hydrogen bond acceptor to Ser31 hydroxyl group, instead the hydrogen bond donor ammonium group in **14** or **18**.

To test an alternative drug binding site near His37 in which the ammonium group can form hydrogen bonds directly with the imidazole rings of His37,[29] docking calculations were performed in the region around the centroid point defined by the four His imidazole nitrogen atoms. The docking poses obtained matched those obtained above using the Am **4** position in the X-ray structure of the complex as reference.

Synopsis: The docking calculations presented here for the interaction of the series of synthetic aminoadamantane derivatives **1**–**18** with the M2TM pore in the 'gas phase' give a mean or chemical interpretation of what is happening inside the binding region, that is, how the apolar and H-bonding interactions are modified for each ligand and change the binding affinity. The binding constants were determined experimentally using the whole M2 protein. In relation to the highly hydrophobic nature of the ligands which appear to have little capacity for different specific interactions with their receptor,[30] the results highlight that experimental binding affinity results from as a delicate compromise between hydrogen bonding and van der Waals interactions on binding.

The binding region inside the symmetric pore includes three apolar levels (HL1, HL2 and HL3 in Fig. 1a) each defined by the four amino acid residues of Val27, Ala30 and Ala34, respectively. This binding surface accommodates the apolar moieties of the studied compounds and its size and shape can be used for designing potential new active ligands than could fill effectively the cavity. In general, Ser31 residues define a key H-bonded interaction with the ammonium group of the ligands. HL3 level corresponds to the most pronounced widening of the apolar cavity allowing sizeable compounds like **8**, **9**, **14** and **18** to cover the space between HL1 and HL3. The calculations locate no binding poses to the wider region above HL3 towards the C-end of the protein.[31]

The gradual increase in binding affinity going from the cyclic amines **1**–**3** or amantadine analogue **5** to amantadine **4** is seems to be the result of the more favourable van der Waals interactions with the symmetric M2TM pore as a result of the increase in symmetry and volume of the ligand's apolar fragment. This is also so for the series of spiranic 2-alkyl-2-adamantanamine analogues **13**, **14**, **18** which have an additional lipophilic segment compared to 2-amantadine **5**, that better fill the available space within the M2TM pore. The relative binding affinities appear to result from a compromise between hydrogen bonding strength and van der Waals enthalpic and entropic contributions as demonstrated from the lowering of binding affinity for the 2-alkyl-2-adamantanamines **10**–**12**. Thus, spiropiperidine **18** covers better the space inside the M2TM pore (Fig. 1e) resulting in the highest binding constant between 2-alkyl-2-adamantanamine series **10**–**18**, but similar to that of amantadine **4** (Fig. 1b), despite stronger van der Waals interactions. It appears that the primary amino group of amantadine which is capable of stronger hydrogen bonding interactions compared to the more crowded secondary amino group of spiropiperidine **18** (i.e., hydrogen bonds with two Ser31 hydroxyl groups and with one Val27 carbonyl group in adjacent chains, compared to one hydrogen bond with Ser31) counteracts the better lipophilic profile of the compound **18**.

Similarly, the relevant docking poses suggest that the much higher binding affinity of rimantadine **7** than amantadine **4** and spiropiperidine **18** should be the result of a better combination of van der Waals and hydrogen bonding interactions (Fig. 1c). The carbon skeleton of rimantadine **7** is more extended than that of amantadine **4** and it is likely that the $CH(CH_3)$ bridge allows the molecule (through free rotation about exocyclic C–$CH(Me)NH_2$ bond) to adopt more easily an orientation permitting a favourable combination of van der Waals and H-bonding interactions. Furthermore, the primary amino group of rimantadine **7** is capable of stronger hydrogen bonding interactions than the secondary amino group of spiropiperidine **18** or the bulky rimantadine analogues **8**, **9**. In addition, the docking calculations predicted a more definite orientation for rimantadine **7**, but many similar docking poses for amantadine and spiropiperidine **18**, consistent with rimantadine **7** forming a more stable complex. In general, for compounds including an

apolar moiety in addition to adamantane (see compounds **8–18**) a fluctuation of the ligand that impairs complex stability is predicted by the docking calculations.

Acknowledgements

This research activity was mainly supported from Chiesi Hellas (elke research project code 10354). A small research grant was also provided by the Special Account for Research Grants of the National and Kapodistrian University of Athens, Greece (research project codes 70/4/5857 and 70/4/8775). This work includes part of Stelios Eleftheratos post-graduate research project.

Supplementary data

Supplementary data associated with this article can be found, in the online version, at doi:10.1016/j.bmcl.2010.05.049.

References and notes

1. Taubenberger, J. K.; Reid, A. H.; Lourens, R. M.; Wang, R.; Jin, G.; Fanning, T. G. *Nature* **2005**, *437*, 889.
2. Wang, T. T.; Palese, P. *Cell* **2009**, *137*, 983.
3. Maines, T. R.; Jayaraman, A.; Belser, J. A.; Wadford, D. A.; Pappas, C.; Zeng, H.; Gustin, K. M.; Pearce, M. B.; Viswanathan, K.; Shriver, Z. H.; Raman, R.; Cox, N. J.; Sasisekharan, R.; Katz, J. M.; Tumpey, T. M. *Science* **2009**, *325*, 484.
4. (a) Ilyushina, N. A.; Bovin, N. V.; Webster, R. G.; Govorkova, E. A. *Antiviral Res.* **2006**, *70*, 121; (b) Jonges, M.; Lubben van der, I. M.; Dijkstra, F.; Verhoef, L.; Koopmans, M.; Meijer, A. *Antiviral Res.* **2009**, *83*, 290.
5. (a) Hay, A. J.; Wolstenholme, A. J.; Skehel, J. J.; Smith, M. H. *EMBO J.* **1985**, *4*, 3021; (b) Hay, A. J. *Semin. Virol.* **1992**, *3*, 21; (c) Pinto, L. H.; Holsinger, L. J.; Lamb, R. A. *Cell* **1992**, *69*, 517; (d) Grambas, S.; Hay, A. J. *Virology* **1992**, *190*, 11.
6. (a) Stouffer, A. L.; Acharya, R.; Salom, D.; Levine, A. S.; Di Costanzo, L.; Soto, C. S.; Tereshko, V.; Nanda, V.; Stayrook, S.; DeGrado, W. *Nature* **2008**, *451*, 596; (b) Cady, S. D.; Schmidt-Rohr, K.; Wang, J.; Soto, C. S.; Degrado, W. F.; Hong, M. *Nature* **2010**, *463*, 689.
7. Pinto, L.; Dieckmann, G. R.; Gandhi, C. S.; Papworth, C. G.; Braman, J.; Shaughnessy, M. A.; Lear, J. D.; Lamb, R. A.; DeGrado, W. F. *Proc. Natl. Acad. Sci. U.S.A.* **1997**, *94*, 11301.
8. Hu, J.; Asbury, T.; Achuthan, S.; Li, C.; Bertram, R.; Quine, J. R.; Fu, R.; Cross, T. A. *Biophys. J.* **2007**, *92*, 4335.
9. Tang, Y.; Zaitseva, F.; Lamb, R. A.; Pinto, L. H. *J. Biol. Chem.* **2002**, *277*, 39880.
10. Pinto, L. H.; Lamb, R. A. *J. Biol. Chem.* **2006**, *281*, 8997.
11. Duff, K. C.; Gilchrist, P. J.; Saxena, A. M.; Bradshaw, J. P. *Virology* **1994**, *202*, 2877.
12. Sansom, M. S.; Kerr, I. D. *Protein Eng.* **1993**, *6*, 65.
13. Khurana, E.; Dal Peraro, M.; DeVane, R.; Vemparala, S.; DeGrado, W. F. *Proc. Natl. Acad. Sci. U.S.A.* **2009**, *106*, 1069.
14. (a) Intharathep, P.; Laohpongspaisan, C.; Rungrotmongkol, T.; Loisruangsin, A.; Malaisree, M.; Decha, P.; Aruksakunwong, O.; Chuenpennit, K.; Kaiyawet, N.; Sompornpisut, P.; Pianwanit, S.; Hannongbua, S. *J. Mol. Graph. Modell.* **2008**, *27*, 342; (b) Laohpongspaisan, C.; Rungrotmongkol, T.; Intharathep, P.; Malaisree, M.; Decha, P.; Aruksakunwong, O.; Sompornpisut, P.; Hannongbua, S. *J. Chem. Inf. Model.* **2009**, *49*, 847.
15. Wang, C.; Takeuchi, K.; Pinto, L. H.; Lamb, R. A. *J. Virol.* **1993**, *67*, 5585.
16. Cady, S. D.; Mishanina, T. V.; Hong, M. *J. Mol. Biol.* **2009**, *385*, 1127.
17. Laughlin, C. A.; Tseng, C. K. Antivirals Agents, RNA Viruses other than HIV. In *Burger's Medicinal Chemistry*, 5th ed., Wolff, M. E., Ed.; John Wiley & Sons: New York, 1997; Vol. 5, pp 571–595
18. For some representative publications see: (a) Kolocouris, A. Ph.D Thesis, National Documentation Center, Vas. Constantinou 48, Athens, Greece, 1995.; (b) Kolocouris, N.; Foscolos, G. B.; Kolocouris, A.; Marakos, P.; Pouli, N.; Fytas, G.; Ikeda, S.; De Clercq, E. *J. Med. Chem.* **1994**, *37*, 2896; (c) Kolocouris, N.; Kolocouris, A.; Foscolos, G.; Fytas, G.; Neyts, J.; Padalko, E.; Balzarini, J.; Snoeck, R.; Andrei, G.; De Clercq, E. *J. Med. Chem.* **1996**, *39*, 3307; (d) Stamatiou, G.; Kolocouris, A.; Kolocouris, N.; Fytas, G.; Foscolos, G. B.; Neyts, J.; De Clercq, E. *Bioorg. Med. Chem. Lett.* **2001**, *11*, 2137; (e) Zoidis, G.; Kolocouris, N.; Foscolos, G. B.; Kolocouris, A.; Fytas, G.; Karayannis, P.; Padalko, E.; Neyts, J.; De Clercq, E. *Antiviral Chem. Chemother.* **2003**, *14*, 153; (f) Stamatiou, G.; Foscolos, G. B.; Fytas, G.; Kolocouris, A.; Kolocouris, N.; Pannecouque, C.; Witvrouw, M.; Padalko, E.; Neyts, J.; De Clercq, E. *Bioorg. Med. Chem.* **2003**, *11*, 5485; (g) Stylianakis, I.; Kolocouris, A.; Kolocouris, N.; Fytas, G.; Foscolos, G. B.; Padalko, E.; Neyts, J.; De Clercq, E. *Bioorg. Med. Chem. Lett.* **2003**, *13*, 1699.
19. Kolocouris, A.; Spearpoint, P.; Martin, S. R.; Hay, A. J.; López-Querol, M.; Sureda, F. X.; Padalko, E.; Neyts, J.; De Clercq, E. *Bioorg. Med. Chem. Lett.* **2008**, *18*, 6156.
20. (a) Kolocouris, A.; Hansen, R.; Broadhurst, R. W. *J. Med. Chem.* **2004**, *47*, 4975; (b) Broadhurst, R. W.; Kolocouris, A.; Zikos, C. *Bioorg. Med. Chem. Lett.* **2007**, *17*, 3947.
21. Czabotar, P. E.; Martin, S. R.; Hay, A. J. *Virus Res.* **2004**, *99*, 57.
22. In the solution NMR structure of a M2 (18–60)–rimantadine complex the drug, in a 200-fold excess, is located on the C-terminus side at helical interfaces, Schnell, J. R.; Chou, J. J. *Nature* **2008**, *451*, 591. This structure seems to represent a non-specific drug binding site model according to the recent ssNMR data, see Ref. 6b.
23. The synthesis of most of the ligands (compounds **6**, **8**, **9**, **13**–**15**, **18**) has been published; experimental details for compounds **10**–**12**, **16**, **17** will be published in the future.
24. See for example: (a) Krumbholz, A.; Schmidtke, M.; Bergmann, S.; Motzke, S.; Bauer, K.; Stech, J.; Dürrwald, R.; Wutzler, P.; Zell, R. *J. Gen. Virol.* **2009**, *9*, 900; (b) Tang, J. W.; Ngai, K. L.; Wong, J. C.; Lam, W. Y.; Chan, P. K. *J. Med. Virol.* **2008**, *80*, 895.
25. Kolocouris, A.; Zell, R. Unpublished data.
26. Astrahan, P.; Kass, I.; Cooper, M. A.; Arkin, I. *Proteins* **2004**, *55*, 251.
27. See for example: (a) Warren, G. L.; Andrews, C. W.; Capelli, A. M.; Clarke, B.; LaLonde, J.; Lambert, M. H.; Lindvall, M.; Nevins, N.; Semus, S. F.; Senger, S.; Tedesco, G.; Wall, I. D.; Woolven, J. M.; Peishoff, C. E.; Head, M. S. *J. Med. Chem.* **2006**, *49*, 5912; (b) Leach, A. R.; Shoichet, B. K.; Peishoff, C. E. *J. Med. Chem.* **2006**, *49*, 5851; (c) Cheng, T.; Li, X.; Liu, Z.; Wang, R. *J. Chem. Inf. Model.* **2009**, *49*, 1079.
28. In contrast recent modelling studies locate no hydrogen bonding for the complex: Du, Q.-S.; Huang, R. B.; Wang, C.-H.; Li, X.-M.; Chou, K.-C. *J. Theor. Biol.* **2009**, *259*, 159.
29. Gandhi, C. S.; Shuck, K.; Lear, J. D.; Dieckmann, G. R.; DeGrado, W. F.; Lamb, R. A.; Pinto, L. H. *J. Biol. Chem.* **1999**, *274*, 5474.
30. Zürcher, M.; Diederich, F. *J. Org. Chem.* **2008**, *73*, 4345.
31. The docking calculations performed on the wild type M2TM sequence of Udorn strain (SSDPLVVAASIIGILHLIL WILDRL) gave similar results; the extra methyl group in residue Ala34 of the mutant sequence (which used for the X-ray structure) seems to assist a little bit aminoadamantane drugs to adopt more stable poses with adamantane orienting towards the wider C-end and ammonium group pointing towards the N-end.